Journal of Crystal Growth 543 (2020) 125699

Contents lists available at ScienceDirect

Journal of Crystal Growth

journal homepage: www.elsevier.com/locate/jcrysgro

# Tuning phase transition kinetics via van der Waals epitaxy of single crystalline $VO_2$ on hexagonal-BN

Saloni Pendse[a], Jie Jiang[a,b], Lifu Zhang[a], Yuwei Guo[a], Zhizhong Chen[a], Yang Hu[a], Zonghuan Lu[c], Songman Li[d], Jing Feng[b], Toh-Ming Lu[c], Jian Shi[a,e,*]

[a] Department of Materials Science and Engineering, Rensselaer Polytechnic Institute, Troy, NY 12180, United States
[b] Faculty of Materials Science and Engineering, Kunming University of Science and Engineering, Kunming 650093, China
[c] Department of Physics, Applied Physics and Astronomy, Rensselaer Polytechnic Institute, Troy, NY 12180, United States
[d] Emma Willard School, Troy, NY 12180, United States
[e] Center for Materials, Devices and Integrated Systems, Rensselaer Polytechnic Institute, Troy, NY 12180, United States

ARTICLE INFO

Communicated by J.M. Redwing

*Keywords:*
A1. Nanostructures
A1. Interfaces
A2. Growth from vapor
B1. Oxides

ABSTRACT

Vanadium dioxide ($VO_2$) is a strongly correlated oxide widely studied for applications in electronics due to its metal-insulator transition at approximately 341 K. While thin films and nanostructures of $VO_2$ have been grown on common rigid substrates like $Al_2O_3$, $TiO_2$, and Si, strong chemical interaction between the substrates and $VO_2$ can induce significant strain during the metal-insulator transition. This not only broadens the temperature range of transition but also leads to the formation of alternating insulating and metallic domains, hence complicating room temperature device applications. Here, we report growth of $VO_2$ wires by conventional as well as van der Waals epitaxy and compare their phase transition dynamics. By revealing metal-insulator transition proceeding via a single domain within a narrow temperature range of 2 K, we present van der Waals epitaxy as an effective tool to tune phase transition kinetics in $VO_2$ or similar systems.

## 1. Introduction

Strongly correlated oxides, with their strong interaction among lattice, charge, orbital and spin degrees of freedom are known to exhibit several intriguing phenomena such as high temperature superconductivity, multiferroicity, colossal magnetoresistance as well as abrupt metal insulator transitions [1–3]. One such oxide, $VO_2$, has long been studied owing to its metal-insulator transition (MIT) [4,5]. The transition, occurring close to room temperature i.e. at 341 K, is accompanied by an electronic/structural phase transition from the low temperature insulating monoclinic (M) phase to the high temperature metallic rutile (R) phase [6,7]. To exploit this transition in functional devices such as sensors, switches and optical shutters, single-crystalline, nanoscale forms of $VO_2$ such as nanowires and nanoplatelets have been developed [8–13].

The one dimensional form of $VO_2$ i.e. nanowires, has especially been sought after since it allows easy tuning of external strain to control electrical and optical properties [11,14,15]. However, most such studies so far have been based on $VO_2$ wires grown on rigid substrates such as $Si/SiO_2$ and sapphire [16–22]. This presents some inherent limitations. Strong chemical interactions (epitaxial or adhesive) between the wire and the substrate in such heterostructures can lead to formation of insulating (M) and metallic (R) domains across the MIT [14,15,23,24]. This broadens the temperature range of transition, hence limiting its room temperature device applications. Furthermore, the exact phase transition characteristics such as appearance and periodicity of new domains can vary from wire to wire depending on factors such as interaction strength of the wire with the substrate, strain non-uniformity along its length as well as its dimensions. This lowers control over MIT kinetics necessary for precise applications.

Recently, there have been efforts to sharpen and better control MIT phase transition dynamics by relaxing the strain at interfaces of such heterostructures. Lee et al. [25] studied sharpening of MIT in $VO_2$ thin film/$TiO_2$ heterostructures by adding a lattice mismatched $SnO_2$ template layer at the interface which relaxed the epitaxial strain and reduced the temperature range of MIT from 20 K to 4 K. Along similar lines, it may be expected that $VO_2$ nanostructures grown on van der Waals (vdW) substrates with negligible interfacial strain and substrate clamping due to the weak nature of vdW interaction, will exhibit a sharpened MIT. This served as the motivation behind the present work as illustrated in Fig. 1. Fig. 1a shows a schematic of phase transition dynamics observed in fully epitaxial $VO_2$ nanostructures grown on rigid

* Corresponding author.
*E-mail address:* shij4@rpi.edu (J. Shi).

https://doi.org/10.1016/j.jcrysgro.2020.125699
Received 29 January 2020; Received in revised form 21 April 2020; Accepted 26 April 2020
Available online 28 April 2020

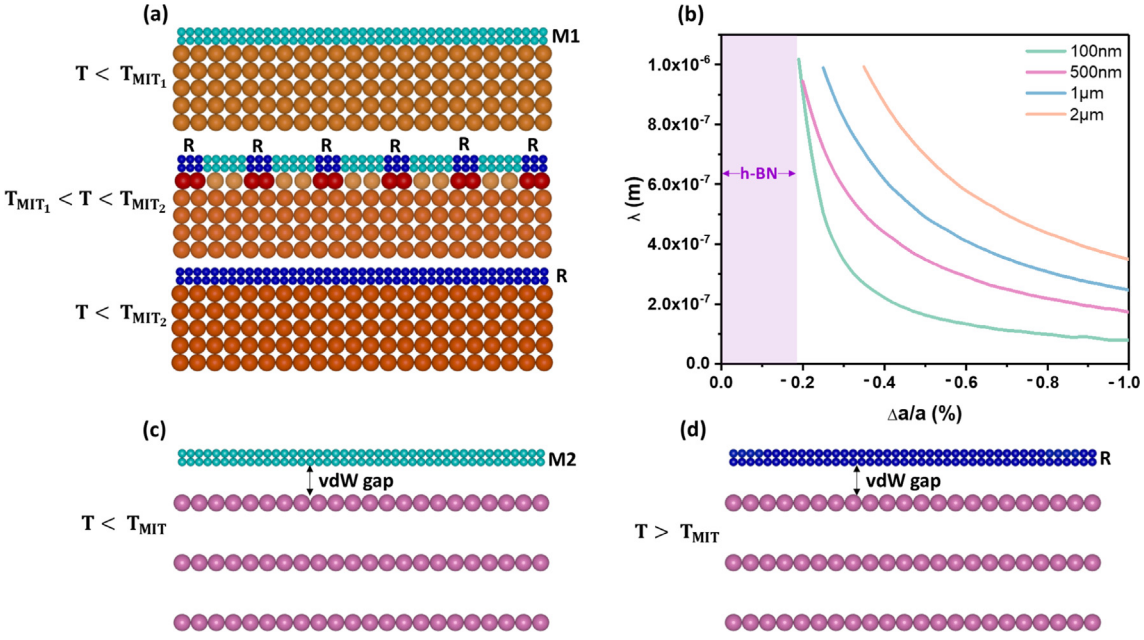


**Fig. 1.** Schematics of metal-insulator phase transition kinetics in $VO_2$. (a) Schematic illustration of MIT in $VO_2$ on a rigid substrate via formation of alternating metallic and insulating domains. (b) Expected domain period (calculated by minimizing Eq. (1). in main text) at a given temperature as a function of induced strain ($\Delta a/a$) due to substrate and wire thickness. (c) & (d) Schematic illustration of MIT in $VO_2$ on a van der Waals substrate via a single domain.

substrates. A transition from insulating (M) to metallic (R) phase involves a 1% contraction along growth direction of the nanostructures ([1 0 0] monoclinic a-axis) [15,23] which is suppressed due to the clamped, epitaxial nature of the wires, hence inducing strain. When heated through the MIT temperature, the transition proceeds by formation of well-distributed and alternating insulating (M) and metallic (R) phases. The fraction of the metallic (R) phase increases with increasing temperature until the phase transformation is complete. At a given temperature, the equilibrium domain period is determined by a trade-off between release of elastic energy resulting from the inherent strain (which favors smaller domain size i.e. placement of tensile and compressive regions in close proximity of one another) and the minimization of domain wall energy (which favors a larger domain size). The overall energy of the nanostructures has been expressed as [15,26,27]:

$$E(\lambda) = \frac{\lambda \epsilon}{\pi^3} \sum_{j=0}^{\infty} \frac{1 - e^{-2(2j+1)\pi t/\lambda}}{(2j+1)^3} + \frac{\gamma t}{\lambda} + \frac{(f_I + f_M)t}{2} \quad (1)$$

where $\lambda$ is the domain period, $\epsilon = Y(\Delta a/a)^2/(1-\vartheta^2)$ is the elastic energy per unit volume, $Y$ is the effective Young's modulus of the system, $\Delta a/a$ is the suppressed lattice contraction along the monoclinic a-axis (or rutile c-axis) during MIT, $\vartheta$ is the Poisson's ratio, $\gamma$ is the domain wall energy per unit domain wall area, $t$ is the nanobeam thickness and $f_M$ and $f_I$ are the free energies of the metallic (R) and the insulating (M) phases respectively. Minimization of Eq. (1) gives the equilibrium domain period at a given temperature and nanobeam thickness. The results are plotted in Fig. 1b for wires of different thickness with $Y = 223$ GPa (average of $Y_{VO_2} = 146$ GPa and $Y_{Al_2O_3} = 306 GPa$ since Eq. (1) assumes an elastically homogeneous system), $\vartheta = 0.2$ and $\gamma = 25$ mJ/m$^2$. It can be seen that for values of strain less than 0.2% (as expected in the case of vdW epitaxy), the expected domain period tends to infinity i.e. the MIT may be expected to proceed instantaneously via a single domain as schematically represented in Fig. 1c and d. Following these arguments, we demonstrate vdW epitaxy-based tuning of phase transition kinetics of $VO_2$ using hexagonal boron nitride (h-BN) as a model vdW substrate that shows excellent thermal stability at $VO_2$ growth temperatures [28].Phase transition dynamics of $VO_2$ wires grown on h-BN are contrasted with those grown by a similar recipe on c-plane sapphire (c-$Al_2O_3$). The epitaxial relation in the $VO_2$/h-BN assembly is reported and a sharpening of the MIT to within 2 K is demonstrated.

## 2. Materials and methods

### 2.1. Materials

Vanadium (IV) oxide powder ($VO_2$, > 99%) was purchased from Sigma Aldrich. The c-plane $Al_2O_3$ and h-BN were purchased from MTI Corp. and HQ Graphene, respectively. As received h-BN crystals were mechanically exfoliated by a scotch tape onto c-$Al_2O_3$ crystals and further used as substrates for growth.

### 2.2. Growth

$VO_2$ wires on c-$Al_2O_3$ and h-BN were grown by a vapor transport method using $VO_2$ as the powder source. $VO_2$ powder and c-$Al_2O_3$ or h-BN substrates were placed in a quartz tube having an outer diameter of 1 in. and loaded into a single-zone horizontal tube furnace. For growth on c-$Al_2O_3$, a procedure adapted from Ref. [21] was followed. Briefly, the source and substrate were placed in close proximity of one another and about 10 cm upstream of the zone center. The furnace was pumped to a base pressure ~1 Torr, after which 30 sccm Ar was flowed in to establish a pressure of 5 Torr. The zone center was then ramped to 873 K within 20 mins and dwelled at 873 K for 3–4 h. After the end of the heating cycle, Ar flow was maintained while the furnace naturally cooled to room temperature. For growth on h-BN, the procedure was slightly modified – the source and substrate were placed about 10 cm apart (in the upstream region), the growth temperature was increased to 923 K and growth time to 10 h. Alternatively, for shorter growth times, the source and h-BN substrates were placed in close proximity (upstream) and the zone center was heated in steps to a higher temperature i.e. first to 923 K where it was dwelled for 20 mins and then to 973 K for 1 h.

### 2.3. Characterizations

A Ti-S Nikon inverted microscope was used for optical microscopy. Raman spectrum was collected with a Renishaw 2000 Raman Spectrometer under a 540 nm laser and a Zeiss 1540 EsB Crossbeam system was used for electron back-scattered diffraction (EBSD) studies. To study the metal-insulator transition, an INSTEC HCS302 temperature stage was used. Samples were glued to the stage with silver paste and images were collected by loading the stage onto the optical microscope. The images were further analyzed for changes in intensity of the wires as a function of temperature during the transition. Intensity of pixels over the wires was determined, averaged and plotted against temperature.

## 3. Results and discussion

Growth of $VO_2$ nanowires from a $VO_2$ source at temperatures much lower than the melting point of $VO_2$ (1815 K) [29] is known to occur via vaporization of $V_2O_5$ (melting point 963 K) [29] from the source. $V_2O_5$ vapor can form due to factors such as - presence of background $O_2$ in the growth environment, presence of $V_2O_5$ as an impurity in the source material or disproportionation of the $VO_2$ source. In brief, the growth mechanism can be described by the following steps – transport of $V_2O_5$ vapor to the substrate, formation of $V_2O_5$ nanodroplets, coalescence, supercooling and loss of oxygen in the slightly reducing environment of the furnace leading to the formation $VO_2$ crystallites and nanowires [29–31]. The resultant epitaxial $VO_2$ wires on c-$Al_2O_3$ and exfoliated h-BN substrates are shown in Fig. 2a and b respectively. Raman spectra of wires grown on h-BN and c-$Al_2O_3$ are shown in Fig. 2c which exhibit clear peaks of $VO_2$ [6], $Al_2O_3$ [32] and h-BN [33]. While the monoclinic $VO_2$ wires on c-$Al_2O_3$ displayed the expected in-plane epitaxial relation $[1\ 0\ 0]||\langle 1\ 1\ \bar{2}\ 0\rangle$ as evidenced by the commonly seen 60° and 120° angles [21], wires on h-BN showed additional angles of 79.1° and 86.9°. To determine the in-plane epitaxial relation of $VO_2$ with respect to h-BN, the orientation of h-BN was determined by EBSD and the results are presented in Fig. 2d. Inverse pole figures show the X and Y direction of h-BN substrate to be [0 1 0] and [1 2 0] respectively. Since the common growth direction of $VO_2$ nanowires on different substrates is known to be rutile [0 0 1] or equivalently monoclinic [1 0 0] [15–17,19–21,34], the observed in-plane epitaxial relations of monoclinic $VO_2$ on h-BN (after conversion to the four-index system) are $[1\ 0\ 0]||\langle 1\ 1\ \bar{2}\ 0\rangle$, $[1\ 0\ 0]||\langle 1\ 4\ \bar{5}\ 0\rangle$ and $[1\ 0\ 0]||\langle \bar{2}\ 7\ \bar{5}\ 0\rangle$. These are highlighted in Fig. 2d. Fig. 2e and f are schematic representations of the observed in plane epitaxial relations of $VO_2$ on c-$Al_2O_3$ and h-BN respectively. Additionally, Fig. 2b and d also provide interesting observations about the growth of $VO_2$ nanostructures in a vdW epitaxy system. The several small $VO_2$ particles seen surrounding the horizontal $VO_2$ nanowires in Fig. 2b are revealed to be vertically growing nuclei in the tilted $VO_2$/h-BN assembly observed in Fig. 2d. Such vertical growth seen on the vdW h-BN substrate but absent on the conventional c-$Al_2O_3$ substrate can be a result of weak vdW bonding at the $VO_2$/h-BN interface. Incoming adatoms during growth may prefer to bond vertically with existing $VO_2$ islands as opposed to aligning on the substrate due to energy considerations [29].

The MIT dynamics in $VO_2$ nanowires grown on c-$Al_2O_3$ and h-BN were studied by optical microscopy facilitated by the sharp optical contrast between the insulating (M) phase and the metallic (R) phase [35] and the results are shown in Fig. 3. Fig. 3a–c show the MIT occurring in nanowires grown on c-$Al_2O_3$. It is clear that the complete transition occurs over a broad temperature window and the dynamics of the phase transition such as nucleation of new domains, domain periodicity and temperature range of transition can vary from one nanowire to another depending on factors such as the exact nature of interaction with the substrate, presence of surrounding features and geometry of growth. Fig. 3d shows MIT in a $VO_2$ nanowire grown on h-BN. The nanowire shown in the figure extends outwards from the h-BN substrate with approximately 10 μm in length directly over the h-BN substrate and undergoes MIT via a single domain over a narrow temperature range within 2 K. Fig. S1 in the Supporting Information shows images of another nanowire on h-BN exhibiting similar MIT characteristics. An analysis of images of wires shown in Fig. 3a and d as a function of temperature during MIT is presented in Fig. 3e. Additional images used for this analysis are presented in Figs. S2 and S3 of the Supporting Information. Comparing the two wires having a thickness of approximately 7 μm, it can be seen that while the intensity of the wire on c-$Al_2O_3$ decreases gradually as more and more metallic (R) domains are created, the intensity of the wire on h-BN decreases instantaneously at 345 K where the transition to the metallic (R) phase proceeds via a

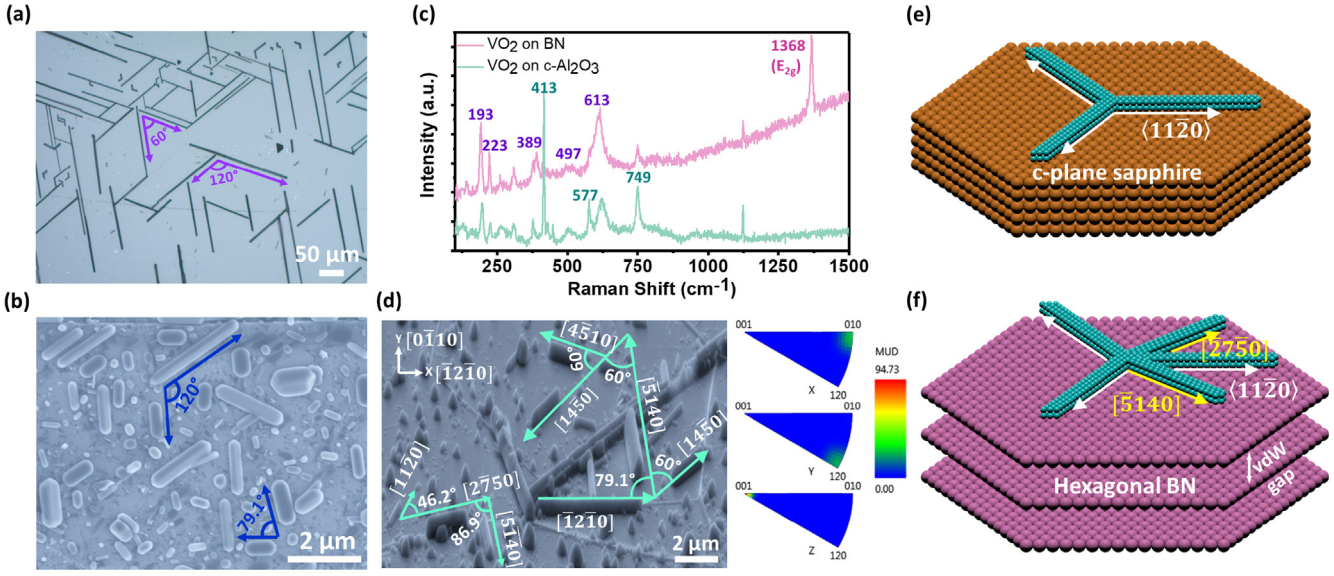


**Fig. 2.** Growth of $VO_2$ on hexagonal boron nitride. (a) Optical microscopy image of $VO_2$ wires grown on c-$Al_2O_3$ (b) SEM image of $VO_2$ wires grown on h-BN. (c) Raman spectra of $VO_2$/h-BN and $VO_2$/c-$Al_2O_3$ assemblies showing distinct peaks of $VO_2$ (highlighted in purple), h-BN (highlighted in pink) and $Al_2O_3$ (highlighted in green). (d) Inverse pole figure of h-BN obtained from EBSD of $VO_2$/h-BN assembly and corresponding SEM image highlighting directions of h-BN along which $VO_2$ wires are seen growing. (e) & (f) Schematic illustrations of epitaxial growth directions of $VO_2$ ([1 0 0] monoclinic or [0 0 1] rutile axis) on c-$Al_2O_3$ and h-BN, respectively.

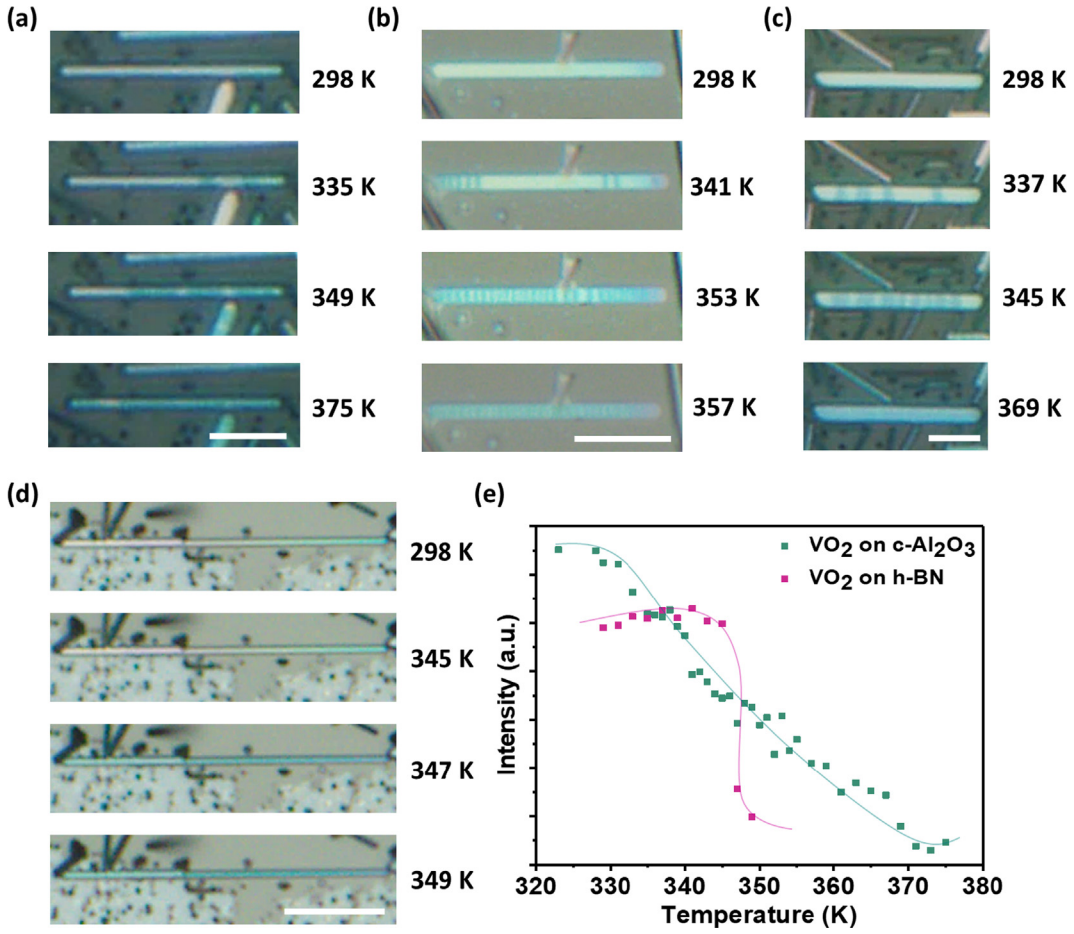


**Fig. 3.** Phase transition kinetics in $VO_2$. (a–c) MIT in $VO_2$ wires grown on c-$Al_2O_3$ proceeding via alternating metallic and insulating domains over a broad temperature range. Scale bars correspond to 5 μm (a & c) and 10 μm (b). (d) MIT in $VO_2$ wires grown on h-BN via a single domain within a temperature range of 2 K. Scale bar corresponds to 10 μm. (e) Analysis of images of $VO_2$ wires shown in (a) and (d) while undergoing MIT.Additional images used in the analysis are presented in Figs. S2 and S3 of the supporting information. Lines have been drawn through the data points to guide the eye.

single domain. Such sharp domain dynamics have been observed only in free standing or suspended $VO_2$ nanobeams so far [8,15]. Hence, absence of periodic domains across the length of the nanowire including the region over h-BN, may be attributed to the weak nature of vdW bonding at the $VO_2$/h-BN interface. The sharpened transition dynamics proceeding via a single domain in epitaxial, on-substrate nanowires can help to better integrate and exploit the near-room-temperature metal-insulator transition exhibited by $VO_2$ in devices.

## 4. Conclusion

In conclusion, vdW epitaxy of $VO_2$ nanowires on h-BN has been demonstrated. The instantaneous and single domain MIT dynamics of $VO_2$ nanowires on h-BN have been studied and contrasted with the broad and less controllable dynamics of epitaxial $VO_2$ nanowires on c-plane sapphire. Such sharpened near-room temperature MIT dynamics in the $VO_2$/h-BN system can facilitate better device functionality. Additionally, with further studies, vdW epitaxy may be extended to other materials systems as an effective tool to tune phase transition kinetics.

## CRediT authorship contribution statement

**Saloni Pendse:** Methodology, Software, Data curation, Writing - original draft. **Jie Jiang:** Methodology, Software. **Lifu Zhang:** Methodology, Software. **Yuwei Guo:** Methodology, Software. **Zhizhong Chen:** Methodology, Software. **Yang Hu:** Methodology, Software. **Zonghuan Lu:** Methodology, Software. **Songman Li:** Methodology, Software. **Jing Feng:** Supervision. **Toh-Ming Lu:** Supervision. **Jian Shi:** Supervision.

## Declaration of Competing Interest

The authors declare that they have no known competing financial interests or personal relationships that could have appeared to influence the work reported in this paper.

## Acknowledgements

We thank Prof. Alexander L. Roytburd from University of Maryland for his insightful discussions. S.P. and J.S. acknowledge the Air Force Office of Scientific Research under award number FA9550-18-1-0116. L.Z. acknowledges the New York State's Empire State Development's Division of Science, Technology and Innovation through Focus Center Contract C150117. Z.C. and Y.H. acknowledge the US National Science Foundation supports under award numbers of 1706815 and 1916652. This material is partially based on work supported by the NSF-MIP Platform for the Accelerated Realization, Analysis, and Discovery of Interface Materials (PARADIM) under cooperative agreement no. DMR-1539918.

## Appendix A. Supplementary material

Supplementary data to this article can be found online at https://

doi.org/10.1016/j.jcrysgro.2020.125699.

## References


[1] J. Mannhart, D.G. Schlom, Oxide interfaces — an opportunity for electronics, Science 327 (2010) 1607–1611, https://doi.org/10.1126/science.1181862.

[2] D. Adler, Mechanisms for metal-nonmental transitions in transition-metal oxides and sulfides, Rev. Mod. Phys. 40 (1968) 714–736, https://doi.org/10.1103/RevModPhys.40.714.

[3] Y.H. Chu, Van der Waals oxide heteroepitaxy, Npj Quantum Mater. 2 (2017) 1–5, https://doi.org/10.1038/s41535-017-0069-9.

[4] F.J. Morin, Oxides which show a metal-to-insulator transition at the neel temperature, Phys. Rev. Lett. 3 (1959) 34–36, https://doi.org/10.1103/PhysRevLett.3.34.

[5] C.N. Berglund, H.J. Guggenheim, Electronic properties of $VO_2$ near the semiconductor-metal transition, Phys. Rev. 185 (1969) 1022–1033, https://doi.org/10.1103/PhysRev.185.1022.

[6] S. Zhang, J.Y. Chou, L.J. Lauhon, Direct correlation of structural domain formation with the metal insulator transition in a $VO_2$ nanobeam, Nano Lett. 9 (2009) 4527–4532, https://doi.org/10.1021/nl9028973.

[7] D. Ruzmetov, S.D. Senanayake, V. Narayanamurti, S. Ramanathan, Correlation between metal-insulator transition characteristics and electronic structure changes in vanadium oxide thin films, Phys. Rev. B– Condens. Matter Mater. Phys. 77 (2008) 1–5, https://doi.org/10.1103/PhysRevB.77.195442.

[8] E. Strelcov, Y. Lilach, A. Kolmakov, Gas sensor based on metal-insulator transition in VO 2 nanowire thermistor, Nano Lett. 9 (2009) 2322–2326, https://doi.org/10.1021/nl900676n.

[9] J.M. Baik, M.H. Kim, C. Larson, C.T. Yavuz, G.D. Stucky, A.M. Wodtke, M. Moskovits, Pd-Sensitized single vanadium oxide nanowires: highly responsive hydrogen sensing based on the metal-insulator transition, Nano Lett. 9 (2009) 3980–3984, https://doi.org/10.1021/nl902020t.

[10] M. Rini, A. Cavalleri, R.W. Schoenlein, R. López, L.C. Feldman, R.F. Haglund, L.A. Boatner, T.E. Haynes, Photoinduced phase transition in VO_2 nanocrystals: ultrafast control of surface-plasmon resonance, Opt. Lett. 30 (2005) 558, https://doi.org/10.1364/ol.30.000558.

[11] B. Hu, Y. Ding, W. Chen, D. Kulkarni, Y. Shen, V.V. Tsukruk, Z.L. Wang, External-strain induced insulating phase transition in $VO_2$ nanobeam and its application as flexible strain sensor, Adv. Mater. 22 (2010) 5134–5139, https://doi.org/10.1002/adma.201002868.

[12] L. Whittaker, C.J. Patridge, S. Banerjee, Microscopic and nanoscale perspective of the metal-insulator phase transitions of $VO_2$: some new twists to an old tale, J. Phys. Chem. Lett. 2 (2011) 745–758, https://doi.org/10.1021/jz101640n.

[13] Z. Yang, C. Ko, S. Ramanathan, Oxide electronics utilizing ultrafast metal-insulator transitions, Annu. Rev. Mater. Res. 41 (2011) 337–367, https://doi.org/10.1146/annurev-matsci-062910-100347.

[14] J. Cao, E. Ertekin, V. Srinivasan, W. Fan, S. Huang, H. Zheng, J.W.L. Yim, D.R. Khanal, D.F. Ogletree, J.C. Grossman, J. Wu, Strain engineering and one-dimensional organization of metal-insulator domains in single-crystal vanadium dioxide beams, Nat. Nanotechnol. 4 (2009) 732–737, https://doi.org/10.1038/nnano.2009.266.

[15] J. Wu, Q. Gu, B.S. Guiton, N.P. De Leon, L. Ouyang, H. Park, Strain-induced self organization of metal-insulator domains in single-crystalline $VO_2$ nanobeams, Nano Lett. 6 (2006) 2313–2317, https://doi.org/10.1021/nl061831r.

[16] B.S. Guiton, Q. Gu, A.L. Prieto, M.S. Gudiksen, H. Park, Single-crystalline vanadium dioxide nanowires with rectangular cross sections, J. Am. Chem. Soc. 127 (2005) 498–499, https://doi.org/10.1021/ja045976g.

[17] C. Cheng, H. Guo, A. Amini, K. Liu, D. Fu, J. Zou, H. Song, Self-assembly and horizontal orientation growth of $VO_2$ nanowires, Sci. Rep. 4 (2014) 1–5, https://doi.org/10.1038/srep05456.

[18] Y. Wang, L. Gao, Y. Yang, Y. Xiang, Z. Chen, Y. Dong, H. Zhou, Z. Cai, G.C. Wang, J. Shi, Nontrivial strength of van der Waals epitaxial interaction in soft perovskites, Phys. Rev. Mater. 2 (2018) 1–8, https://doi.org/10.1103/PhysRevMaterials.2.076002.

[19] L. Wang, H. Ren, S. Chen, Y. Chen, B. Li, C. Zou, G. Zhang, Y. Lu, Epitaxial Growth of well-aligned single-crystalline $VO_2$ Micro/Nanowires Assisted by Substrate Facet Confinement, Cryst. Growth Des. 18 (2018) 3896–3901, https://doi.org/10.1021/acs.cgd.8b00212.

[20] S.V. Mutilin, V.Y. Prinz, V.A. Seleznev, L.V. Yakovkina, Growth of ordered arrays of vertical free-standing $VO_2$ nanowires on nanoimprinted Si, Appl. Phys. Lett. 113 (2018), https://doi.org/10.1063/1.5031075.

[21] J.I. Sohn, H.J. Joo, A.E. Porter, C.J. Choi, K. Kim, D.J. Kang, M.E. Welland, Direct observation of the structural component of the metal-insulator phase transition and growth habits of epitaxially grown $VO_2$ nanowires, Nano Lett. 7 (2007) 1570–1574, https://doi.org/10.1021/nl070439q.

[22] J.I. Sohn, H.J. Joo, D. Ahn, H.H. Lee, A.E. Porter, K. Kim, D.J. Kang, M.E. Wellandt, Surface-stress-induced Mott transition and nature of associated spatial phase transition in single crystalline $VO_2$ nanowires, Nano Lett. 9 (2009) 3392–3397, https://doi.org/10.1021/nl900841k.

[23] Alexander Tselev, Evgheni Strelcov, Igor A. Luk'yanchuk, John D. Budai, Jonathan Z. Tischler, Ilia N. Ivanov, Keith Jones, Roger Proksch, Sergei V. Kalinin, Andrei Kolmakov, Interplay between ferroelastic and metal – insulator phase transitions in strained quasi-two-dimensional $VO_2$ nanoplatelets, Nano Lett. 10 (6) (2010) 2003–2011, https://doi.org/10.1021/nl1008794.

[24] J. Wei, Z. Wang, W. Chen, D.H. Cobden, New aspects of the metal-insulator transition in single-domain vanadium dioxide nanobeams, Nat. Nanotechnol. 4 (2009) 420–424, https://doi.org/10.1038/nnano.2009.141.

[25] D. Lee, J. Lee, K. Song, F. Xue, S.Y. Choi, Y. Ma, J. Podkaminer, D. Liu, S.C. Liu, B. Chung, W. Fan, S.J. Cho, W. Zhou, J. Lee, L.Q. Chen, S.H. Oh, Z. Ma, C.B. Eom, Sharpened $VO_2$ phase transition via controlled release of epitaxial strain, Nano Lett. 17 (2017) 5614–5619, https://doi.org/10.1021/acs.nanolett.7b02482.

[26] A.L. Roytburd, Thermodynamics of polydomain heterostructures. I. Effect of macrostresses, J. Appl. Phys. 83 (1998) 228–238, https://doi.org/10.1063/1.366677.

[27] S.P. Alpay, A.L. Roytburd, Thermodynamics of polydomain heterostructures. III. Domain stability map, J. Appl. Phys. 83 (1998) 4714–4723, https://doi.org/10.1063/1.367260.

[28] N. Kostoglou, K. Polychronopoulou, C. Rebholz, Thermal and chemical stability of hexagonal boron nitride (h-BN) nanoplatelets, Vacuum 112 (2015) 42–45, https://doi.org/10.1016/j.vacuum.2014.11.009.

[29] E. Strelcov, A.V. Davydov, U. Lanke, C. Watts, A. Kolmakov, In situ monitoring of the growth, intermediate phase transformations and templating of single crystal $VO_2$ nanowires and nanoplatelets, ACS Nano. 5 (2011) 3373–3384, https://doi.org/10.1021/nn2007089.

[30] M.H. Kim, B. Lee, S. Lee, C. Larson, J.M. Baik, C.T. Yavuz, S. Seifert, S. Vajda, R.E. Winans, M. Moskovits, G.D. Stucky, A.M. Wodtke, Growth of metal oxide nanowires from supercooled liquid nanodroplets, Nano Lett. 9 (2009) 4138–4146, https://doi.org/10.1021/nl902357q.

[31] Y. Cheng, T.L. Wong, K.M. Ho, N. Wang, The structure and growth mechanism of $VO_2$ nanowires, J. Cryst. Growth. 311 (2009) 1571–1575, https://doi.org/10.1016/j.jcrysgro.2009.01.002.

[32] G.H. Watson, W.B. Daniels, C.S. Wang, Measurements of Raman intensities and pressure dependence of phonon frequencies in sapphire, J. Appl. Phys. 52 (1981) 956–958, https://doi.org/10.1063/1.328785.

[33] Q. Cai, D. Scullion, A. Falin, K. Watanabe, T. Taniguchi, Y. Chen, E.J.G. Santos, L.H. Li, Raman signature and phonon dispersion of atomically thin boron nitride, Nanoscale 9 (2017) 3059–3067, https://doi.org/10.1039/c6nr09312d.

[34] Y. Wang, X. Sun, Z. Chen, Z. Cai, H. Zhou, T.M. Lu, J. Shi, Defect-engineered epitaxial $VO_2 \pm$ d in strain engineering of heterogeneous soft crystals, Sci. Adv. 4 (2018) 1–11, https://doi.org/10.1126/sciadv.aar3679.

[35] B. Fisher, Metal-semiconductor domain configurations during switching of VO 2 single crystals, J. Phys. C Solid State Phys. 9 (1976) 1201–1209, https://doi.org/10.1088/0022-3719/9/7/011.